Jurnal Ilmu Fisika
Vol. 16, No. 2, September 2024, pp. 107–117
ISSN: 1979-4657 (Print); 2614-7386 (Online)
https://doi.org/10.25077/ 10.25077/jif.16.2.107-117.2024

Jurnal Ilmu Fisika
Open Access

Validation of OpenMC Code for Low-cycle and Low-particle Simulations in the Neutronic Calculation

Ahmad Muzaki Mabruri[1], Ratna Dewi Syarifah[2], Indarta Kuncoro Aji[3], Artoto Arkundato[2], Nuri Trianti[4]

[1] Department of Nuclear Science and Engineering, Bandung Institute of Technology, Bandung, 40132, Indonesia
[2] Department of Physics, Faculty of Mathematics and Natural Sciences, University of Jember, Jember, 68121, Indonesia
[3] Molten Salt Lab. Inc., UEC Alliance Center, 1-1 Kojimacho, Chofu, Tokyo, 182-0026, Japan.
[4] Research Center for Nuclear Reactor Technology ORTN, BRIN, Serpong, 15314, Indonesia

Article Info

Article History:

Received February 07, 2024
Revised April 07, 2024
Accepted April 20, 2024
Published online May 19, 2024

Keywords:

Criticality
k-eff
Low-cycle
MSR FUJI-12
OpenMC

Corresponding Author:

Ratna Dewi Syarifah,
Email: rdsyarifah.fmipa@unej.ac.id

ABSTRACT

Validation of Low-Cycle and Low-Particle OpenMC Simulation Codes for Neutronics Calculations has been conducted. This study validates OpenMC, an evolving open-source neutron analysis code. Validation of Low-Cycle and Low-Particle Codes is crucial as it allows for effective calculations with minimal computational resources. Determining the convergence point of cycles and minimum particles in low-cycle and low-particle calculations enables maintaining calculation accuracy, thus providing sufficiently accurate results. This study demonstrates that a minimum of 15,000 particles, 100 cycles (30 inactive, 70 active), is required for low-cycle simulations. A comparison of k-eff calculation results with the SRAC code for MSR FUJI-12 at 7 burnup points (0-27 MWd/ton) yields a maximum error of 0.7%. These results validate the effectiveness of OpenMC in achieving accurate neutronic calculations with limited computational resources.

1. INTRODUCTION

The Molten Salt Reactor (MSR) is a nuclear reactor with both its fuel and coolant in the form of a molten salt solution. The fuel for an MSR can be uranium, plutonium, or thorium dissolved in molten salt (Yamaguchi et al., 2017).The liquid phase of the fuel solution is maintained by ensuring the solution is at the eutectic mixing point, operating at low pressure and high temperature (Yamaguchi et al., 2017; Souček et al., 2018). The MSR FUJI-12 is a design of MSR developed by Japan, which is relatively small compared to similar reactors. The MSR FUJI-12 is designed with a single homogeneous core, as shown in Figure 1, and commonly utilizes a mixture of molten salts such as LiF-BeF_2-ThF_4-UF_4 as fuel (Waris et al., 2012).

The use of nuclear technology as a nuclear power plant must go through a very comprehensive analysis. Neutronic analysis is a critical analysis related to the interaction of neutrons in the reactor core. Neutrons are the primary atomic particles in reactors that can cause fission reactions, so it is essential to know the behavior of neutrons in order to obtain a safe and neutronically optimal reactor design

(Syarifah et al., 2021; Karomah et al., 2023). Neutronic analysis can be simulated with several compatible analysis codes such as SRAC, MCNP, SERPENT, and ORIGENT. Each code has a different calculation method and accuracy, so more than one code is needed to conclude an optimal reactor design.

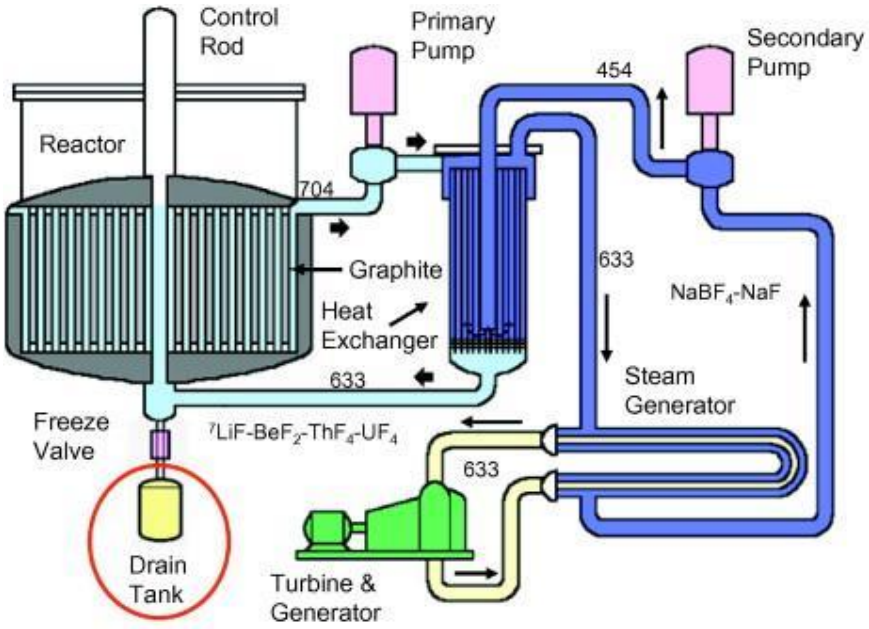

Figure 1. FUJI-12 MSR Design (IAEA, 2016)

OpenMC is a neutronic analysis code developed by Computational Reactor Physics Group members from the Massachusetts Institute of Technology in 2011. This code is open source and continues to be developed by many researchers around the world. OpenMC is a code based on Monte Carlo simulation with geometry modeling based on the Constructive Solid Geometry method. OpenMC is capable of calculating fixed-source neutron and photon transport, *k*-eigen calculations, reactor criticality, and CAD calculations. In addition, OpenMC is also able to support multigroup or continuous transportation of energy and particles (Romano et al., 2015; OpenMC, 2023). This code is counted as a new code in neutronic analysis, so it needs to be validated with other codes so that it can become a reference in the use of nuclear technology.

Convergence of neutron source distribution is crucial to validate Monte Carlo-based neutron transport calculations such as OpenMC. The neutron source distribution is related to the behavior of neutron interactions; thus, ensuring a converged neutron distribution is essential to obtain neutron interaction histories representative of the entire modeled reactor core. A simple way to achieve this state is by increasing the number of cycles and neutron histories during calculations. However, this method could be more efficient as it requires high computational resources and can lead to lengthy simulation durations**.**

Shanon entropy is a calculation method used to determine the convergence of neutron distribution within a specific mesh. The geometry is divided into several meshes, and the number of neutrons distributed in each mesh is identified to determine the value of Shanon entropy. This method has been utilized, among others, in determining the convergence of neutron sources in the MCNP code by Farkas et al. (2017). The results of this study indicate that the neutron distribution becomes more convergent with a larger number of neutron histories. The number of cycles also determines how converged the neutron distribution is. However, it is observed that there is a minimum cycle required to reach a stationary state in the neutron distribution for each cycle (Farkas et al., 2017).

The stationary point distribution of the neutron source needs to be determined to minimize the error value in Monte Carlo calculations. The stationary point is marked as the starting point of the active

cycle, and the inactive neutron distribution point marks the part of the neutron distribution that has not yet converged. Determining the number of inactive cycles is important to perform effective calculations using Monte Carlo (Brown, 2006). Research conducted by Hursin et al., 2024, shows that the distribution of neutrons in each cycle can be different, so the results of the analysis of the neutron distribution in each cycle can be different. Based on this, apart from influencing the criticality parameter (*k-eff*), the distribution of neutrons can directly influence the flux parameters, fission rate, and other physical parameters.

This research validates the results of neutronic analysis of OpenMC calculations for calculations with a small number of particles and cycles. Validation is carried out by calculating the entropy value of the neutron source distribution in order to obtain the minimum number of cycles for converging source simulations. The number of particles is varied and then used to estimate calculations that have been carried out on the *k-eff* data reference source from SRAC calculations for MSR FUJI-12. The SRAC code was chosen because it uses a deterministic calculation system with a diffusion equation approach different from the OpenMC system. In addition, SRAC has been validated and used for neutronic analysis of nuclear reactors for a long time (Kumala Sari et al., n.d.; Syarifah et al., 2017a, 2017b, 2018, 2020, 2022). Validation is carried out by comparing the k-eff value of fuel burn-up results from the two codes. The *k-eff* value is an important parameter to indicate neutron production activity in the reactor (Syarifah et al., 2024). Controlling *k-eff* is important in neutronic safety, so the code must be able to calculate the correct k-eff.

2. METHOD

2.1 Calculation of eigenvalues (*k*)

Reactor criticality calculations by OpenMC cannot be separated from the neutron transport equation. The neutron transport equation shows that the change in the rate of neutron density is proportional to the number of absorbed and leaked neutrons.

$$\frac{1}{v}\frac{\partial}{\partial t}\psi\left(\boldsymbol{r},\boldsymbol{\Omega},E,t\right)+\boldsymbol{\Omega}.\nabla\psi\left(\boldsymbol{r},\boldsymbol{\Omega},E,t\right)+\Sigma_t\left(\boldsymbol{r},E\right)\psi((\boldsymbol{r},\boldsymbol{\Omega},E,t)=\ q_{ext}\left(\boldsymbol{r},\boldsymbol{\Omega},E,t\right)+$$
$$+\int_{4\pi}d\boldsymbol{\Omega}'\int_0^\infty dE'\Sigma_s(\boldsymbol{r},\boldsymbol{\Omega}'\rightarrow\boldsymbol{\Omega},E'\rightarrow E)\psi\left(\boldsymbol{r},\boldsymbol{\Omega}',E',t\right)+ \quad (1)$$
$$+\frac{\chi\left(\boldsymbol{r},E\right)}{4\pi}\int_{4\pi}d\boldsymbol{\Omega}'\int_0^\infty dE'\nu\left(\boldsymbol{r},E'\right)\Sigma_f\left(\boldsymbol{r},E'\right)\psi\left(\boldsymbol{r},\boldsymbol{\Omega}',E',t\right)$$

By formulating equation 1 in a steady state and adding the eigenvalue (*k*) from dividing $\nu(\boldsymbol{r},E')$ with *k*, Equation (2) is obtained (Mickus, 2021; Mabruri et al., 2022).

$$\boldsymbol{\Omega}.\nabla\psi\left(\boldsymbol{r},\boldsymbol{\Omega},E\right)+\Sigma_t\left(\boldsymbol{r},E\right)\psi\left(\boldsymbol{r},\boldsymbol{\Omega},E\right)=\int_{4\pi}d\boldsymbol{\Omega}'\int_0^\infty dE'\Sigma_s(\boldsymbol{r},\boldsymbol{\Omega}'\rightarrow\boldsymbol{\Omega},E'\rightarrow E)\psi\left(\boldsymbol{r},\boldsymbol{\Omega}',E'\right)+$$
$$+\frac{1}{k}\frac{\chi\left(\boldsymbol{r},E\right)}{4\pi}\int_{4\pi}d\boldsymbol{\Omega}'\int_0^\infty dE'\nu\left(\boldsymbol{r},E'\right)\Sigma_s\left(\boldsymbol{r},E'\right)\psi\left(\boldsymbol{r},\boldsymbol{\Omega}',E'\right) \quad (2)$$

The Monte Carlo method is a method of solving deterministic problems with a stochastic approach using random numbers. A number of n independent observations (e.g. neutron history) are collected to solve a difficult deterministic problem by obtaining the average of the observations. The advantage of the Monte Carlo method is that it can solve complex problems without simplification. Very complex problems can be solved with very accurate solutions by doing more repetitions (more observations) and by increasing the number of *n* samples. This is guaranteed by the central limit theorem (Vaz, 2009; Kunlun, 2016). The use of the Monte Carlo method in the neutron transport simplifies

Equation (2) into a Monte Carlo iteration form by creating an operator ***S*** which is a source of fission and ***F*** which is the fission operator (Carney et al., 2014; Mickus, 2021), so that it is obtained:

$$S^{i+1} = \frac{1}{k^i} \boldsymbol{F} \boldsymbol{S}^{\boldsymbol{i}} \tag{3}$$

$S^{(i)}$ denotes a sample of the neutrons at their current state, whereas $S^{(i+1)}$ show the next generation of neutrons. Iteration starts from the initial state $S^{(0)}$ with eigenvalues $k^{(0)}$.

2.2 Entropy convergence

The entropy value of the source distribution can be determined by determining the 3D-mesh that divides the geometry of the reactor core. The total mesh must cover the entire fission zone area to limit source leakage. The fraction of the fission site in each mesh can be determined by the following equation:

$$S_i = \frac{\text{Source sites in } i-\text{th mesh element}}{\text{Total number of source sites}} \tag{4}$$

with $i = 1,2,3,,,,N$ denotes the i-th mesh. The entropy value can be calculated by discretizing the problem space into N regions. In each region i, the fraction of fission source neutrons (S_i) in that region is calculated, so the estimation of Shannon entropy can be determined by Equation (5) (Kiedrowski & Beyer, 2017; Omar, 2021; OpenMC, 2023):

$$H = -\sum_{i=1}^{N} S_i \log_2 S_i \tag{5}$$

where N is the number of meshes.

In this study, the FUJI-12 MSR core shown in Figures 2 and 3 will be divided into an 8x8x8 3D mesh. The number of scattered neutron sources in each mesh is identified and then calculated using equation 5 to obtain the entropy value. The active cycle point is then evaluated based on the initial point of the stationary state that can be achieved by all variations of neutron history from 15,000 to 1,000,000. The stationary point is evaluated based on the initial point of fluctuation with a uniform state. Meanwhile, the minimum number of particles is determined based on calculating the *k-eff* value from all variations in the number of particles. The point where *k-eff* begins to converge on variations in the number of particles simulated used as a reference for low-particle calculations.

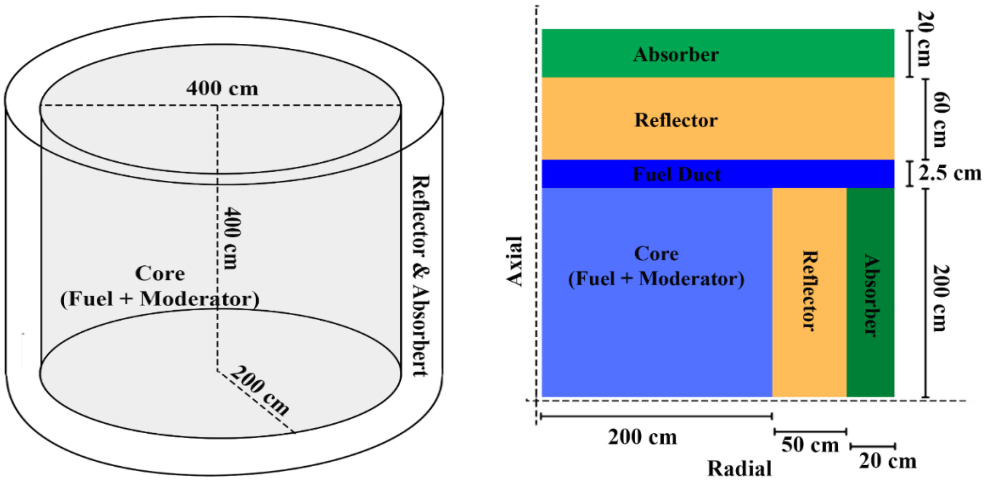

(a) (b)

Figure 2. Reactor core model (a) shape of the reactor core and (b) the configuration of the core material.

2.3 Design and Parameters

MSR FUJI-12 has a cylindrical core shape with one core, and is covered by reflector and absorber layers on the axial and radial sections. In addition, there is a fuel duct to the cooler called the fuel duct between the core and reflector in the axial direction. The MSR FUJI-12 model in this study refers to the design shown in Figure 2. The specifications of the components making up the reactor core and the fuel used are described in Table 1.

Table 1. Core material specifications (Waris et al., 2012, 2015)

Parameter	Value
Fuel	71.78% LiF 16.00% BeF_2 12.00% ThF_4 0.32% UF_4
Density	2.9 gr/cm^3
Thermal output	840 Kelvin
Moderator	Graphite (C)
Density	1.84 g/cm^3
Reflector	Graphite (C)
Density	1.76 g/cm^3
Absorber	Boron Carbide (CB_4)
Density	2.52 g/cm^3

Figure 3 is the hexagonal lattice configuration of the graphite and fuel moderator on the MSR FUJI-12. According to (Suzuki & Shimazu, 2008), the volume fraction of graphite moderators in the core is 70%, so the number of hexagonal lattices required is 271. Figure 3 is a lattice size specification commonly used on the MSR FUJI-12. It requires ten hexagonal lattice rings to model the MSR FUJI-12 according to the moderator fraction value.

Operation MSR FUJI-12 is operated according to the operating parameters shown in Table 2. The reactor was operated for five years with a maximum total fuel burn-up of 27 MWd/Ton. Operating power is set to work at 350MWt for all burn-up points. Other operating parameters can be seen in Table 2.

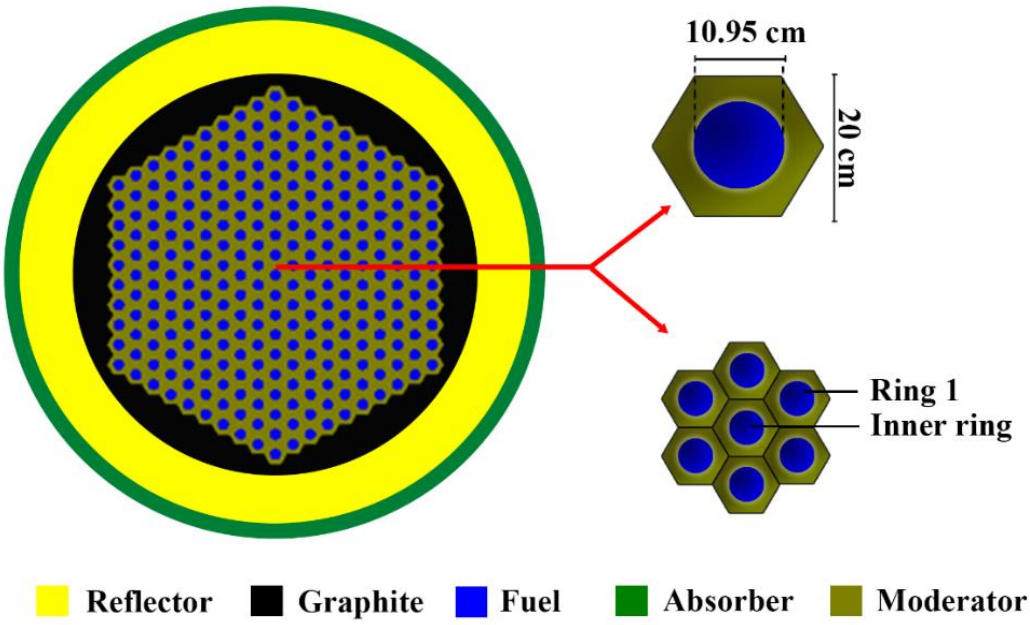

Figure 3. Hexagonal lattice configuration.

Table 2. Operating parameters of the MSR FUJI-12 reactor (Waris et al., 2012)

Parameter	Specification
Thermal Power	350 MWt
Electric Power	150 Mwe
Inlet Temperature	840 Kelvin
Outlet Temperature	980 Kelvin
Refueling Period	5 years
Avg. Power Density	7 Sec/liter
Burn-up Point	(2.7, 5.4, 8.1, 13.5, 18.9, 24.3, 27.0) MWd/Ton

Criticality simulation of the reactor is carried out by dividing the maximum burn-up of 27 MWd/Ton into seven burn-up points. This setup determines the characteristics of changes in the value of *k-eff* from the beginning to the end of the burn-up. These are also reference points for validating the *k-eff* value according to the calculation of the SRAC code simulation.

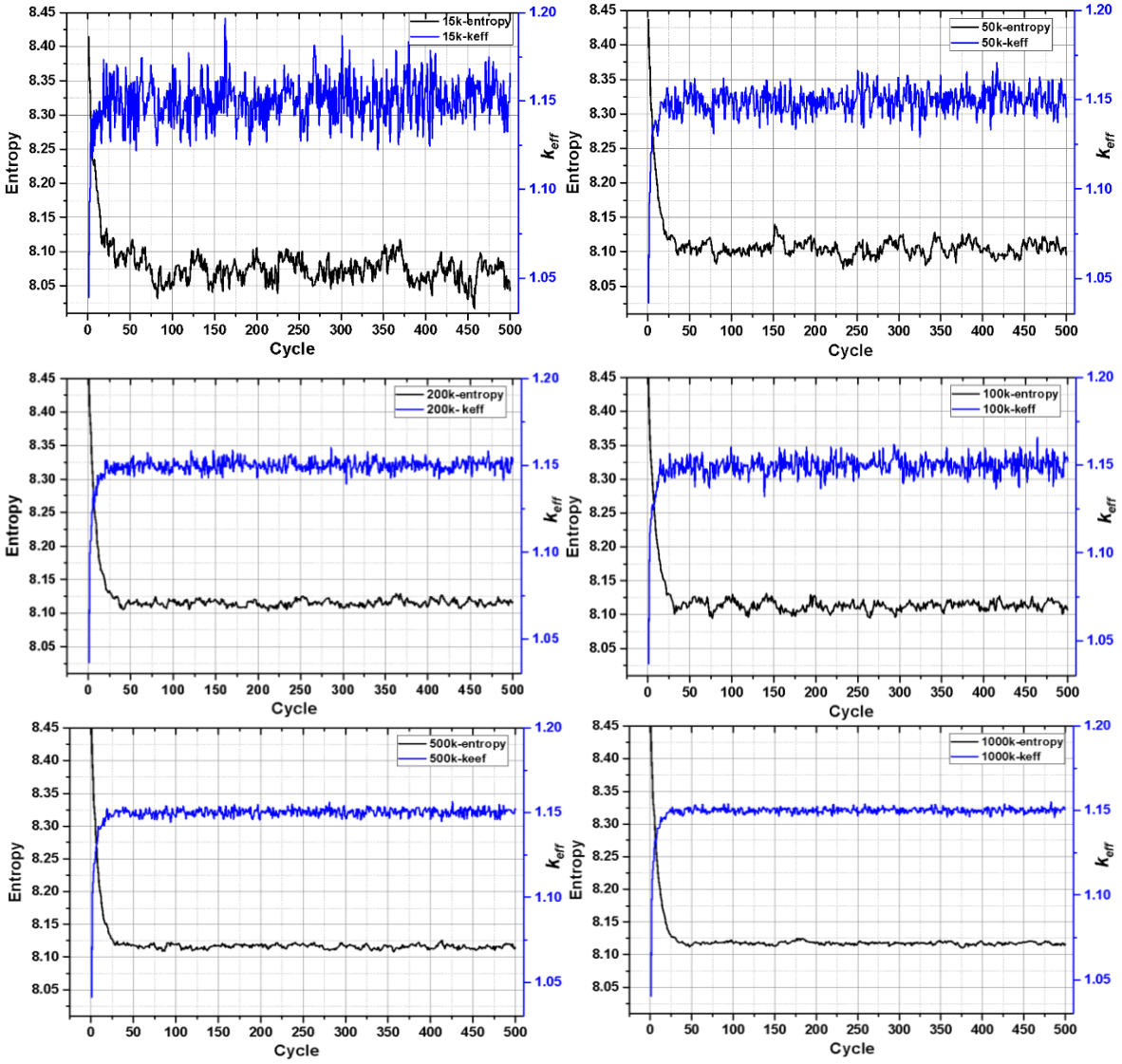

Figure 4. Convergence of *k-eff* and entropy.

3. RESULTS AND DISCUSSION

The results of calculating k-eff and entropy with 500 active cycles have been carried out with the results shown in Figure 4. The results show that the convergence characteristic of *k-eff* and entropy values starts at cycle 30 and above (cycle > 30) for all variations in the number of particles used. It can be seen that fluctuations in entropy and *k-eff* values occur at the 30 – 500 cycle point. The higher the number of simulated particles, the more minor the fluctuations in *k-eff* and entropy values (Brown, 2006; Carney et al., 2014; Kunlun, 2016). Entropy indicates the level of neutron source distribution in the reactor core geometry. It is crucial to obtain the correct particle behavior data to obtain *k-eff*. The larger the simulated particles, the more evenly distributed the neutron sources in the reactor design are, resulting in a more accurate *k-eff* (Farkas et al., 2017).

The final value of the *k-eff* calculation for all variations in the number of particles is shown in Table 3. Based on Figure 4, the results of the simulation calculations can be grouped into low, medium, and high. The final result of the *k-eff* value for each variation is close to *k-eff* ≈1.1500. The difference between the variations is the level of accuracy. The high group has inaccuracies (accuracy errors) below 10 pcm, while the medium and low groups are above 10 pcm. The number of cycles also affects the *k-eff* value error; the larger the cycle used, the smaller the calculation error obtained.

Table 3. Calculation value of *k-eff*

Particles (N)	$k_{eff} \pm error$	Group Particle
15K	1.1498± 0.00037	Low ($N < 50K$)
50K	1.1495± 0.00021	
100K	1.1497± 0.00015	Medium ($50K < N < 500K$)
200K	1.1499± 0.00011	
500K	1.1500± 0.00007	High ($N > 500K$)
1000K	1.1499± 0.00006	

The results of the entropy validation in Figure 4 show that active cycles can start at cycle 31 or more. Based on these results, a *k-eff* calculation is simulated with a lower number of cycles (low-cycle). Figure 5 is the simulation result of variations in the number of particles from 100 – 1,000,000, with 100 cycles consisting of 30 inactive and 70 active cycles. The 31st cycle point was chosen as the start of the active cycle calculation based on the entropy convergence data in Figure 4. The calculation results in Figure 5 show that the fluctuations in the *k-eff* value decrease in the particle range of 10,000 – 1,000,000.

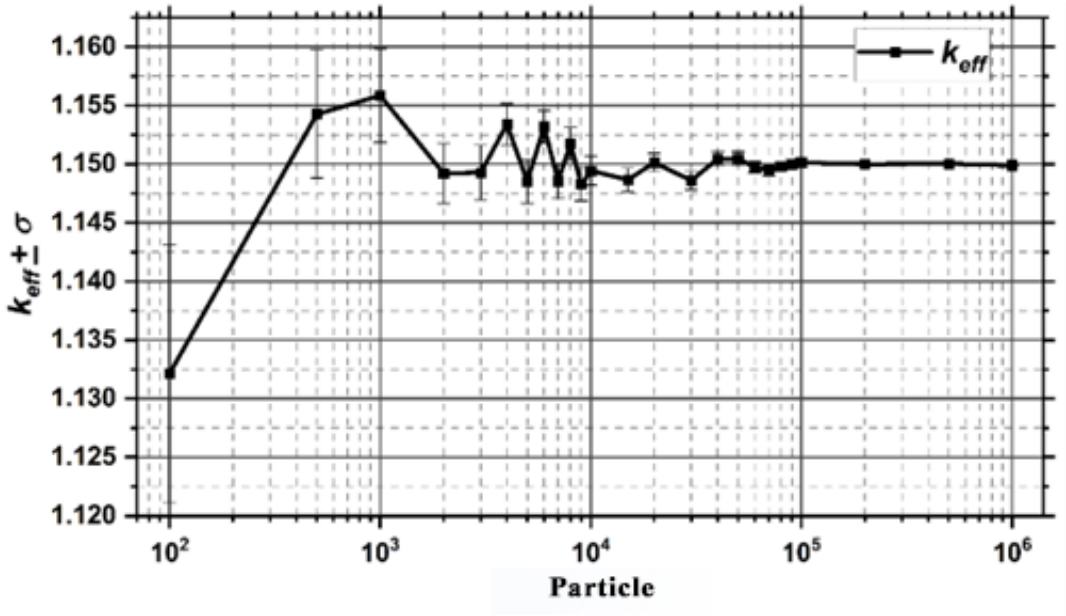

Figure 5. *K-eff* value for the number of particles.

Based on the results in Figure 5, 15,000 particles are used as a reference for calculating low particles. Figure 6 is the result of a comparison of the simulation results of OpenMC and SRAC *k-eff* calculations. The comparison results are intended to show the level of precision of OpenMC calculations against SRAC calculations. The low cycle uses 15,000 particles with 100 cycles, while the high cycle uses 200,000 particles with 500 cycles. Comparisons were made for seven fuel burn-up points in the 0 – 27 MWd/ton range.

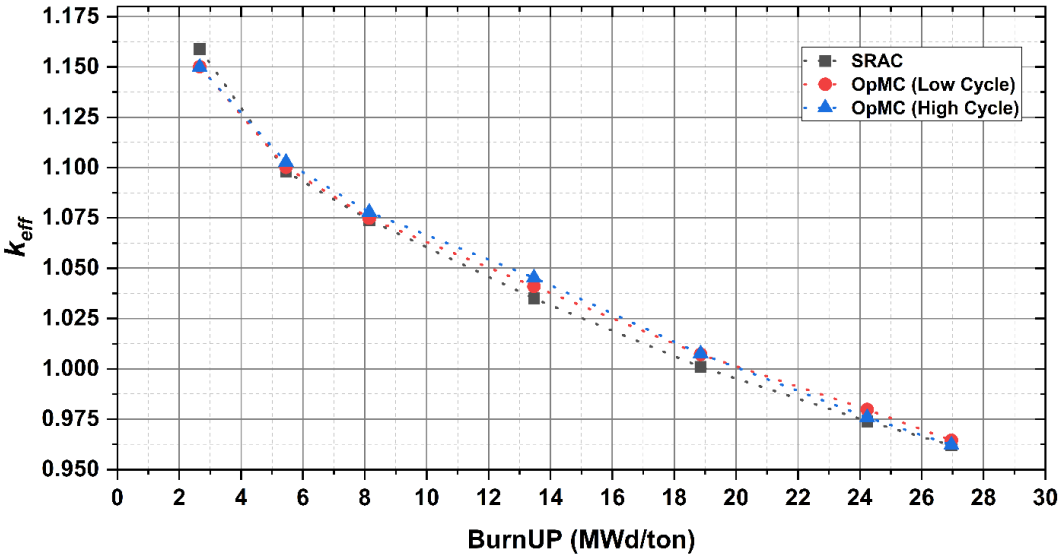

Figure 6. Validation of SRAC and OpenMC.

Based on the results in Figure 6, compared with the results of research by Waris et al. (2012), the largest error value for the comparison of low cycle and high cycle with SRAC after a burn-up process of 0 – 27 MWd/ton is 0.7%. It shows that the level of precision of the two codes for the SRAC calculation is 99.3%. This value can be precise and can be used to state that the *k-eff* calculation by OpenMC has been validated based on SRAC data references. In addition, these results also show that the low-cycle OpenMC simulation is sufficient to obtain a precise *k-eff* value.

Table 4. Physical parameter analysis value.

Physical Parameter	**Low-Cycle (LC)**	**High-Cycle (HC)**	$\frac{\lvert HC - LC \rvert}{HC} \times 100$
Fission Rate	0.461129 ± 0.000721947	0.460334 ± 5.92E-05	0.17%
Nu-Fission Rate	1.15186 ± 0.00180282	1.14987 ± 0.000148	0.17%
Flux	251.502 ± 0.129979	251.484 ± 0.014017	0.01%
Total Reaction Rate	101.043 ± 0.0550079	101.034 ± 0.005936	0.01%
Heating	8.18E+07 ± 125336	8.16E+07 ± 10265.3	0.17%
Heating-Local	9.07E+07 ± 136628	9.05E+07 ± 11203.7	0.17%

In addition to the *k-eff* calculation, there is output for calculating physical parameters that can be issued by OpenMC according to the tallies and score settings used. The physical parameter values can be seen in Table 4, which shows the average reaction value of the 1-energy group (0-200 MeV). The difference between the Low-Cycle and High-Cycle calculation st.dev error values for each physical parameter is evident. High-Cycle calculations have st.dev error values ten times smaller than Low-Cycle calculations. This condition shows that the High-cycle is ten times more accurate than the Low-cycle. Meanwhile, the difference in the results of calculating the physical parameters is 0.01% for the flux and

total reaction values and 0.17% for the other parameters. Based on these results, the precision level of the Low-cycle calculation to the High-Cycle calculation is 99.83% - 99.99%.

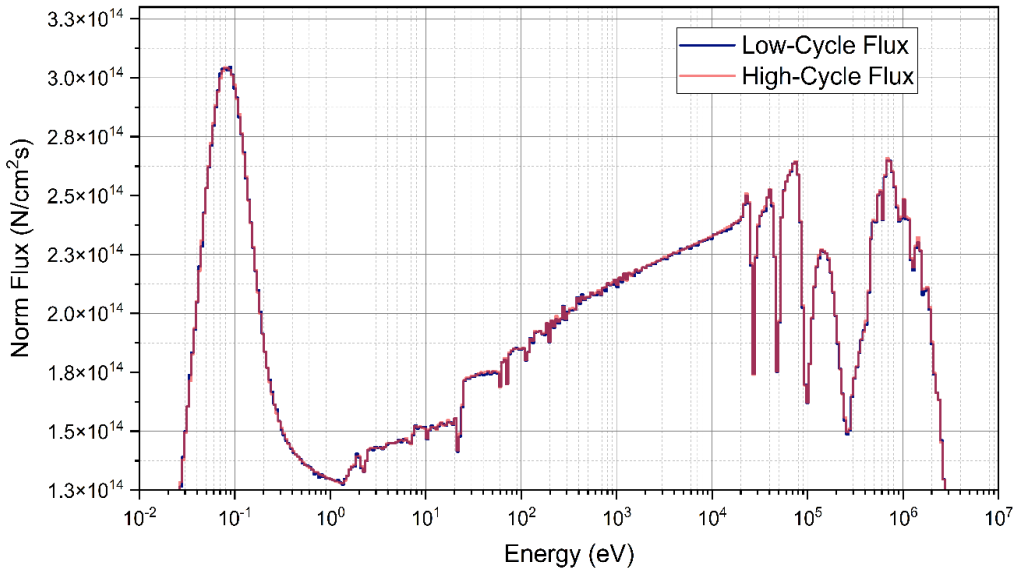

Figure 7. Validation of SRAC and OpenMC.

Figure 7 compares the flux spectra from the High-cycle and Low-cycle calculations. The neutron flux is related to neutrons' behavior while in the nucleus. Flux shows the total distribution of reactions that cause an increase or decrease in neutrons in the reactor core during reactor operation. Figure 7 shows the distribution of neutron flux values based on 500 energy groups 0 – 200 MeV. This reactor is a type of thermal reactor based on its peak spectrum. The comparison results between High-cycle and Low-cycle simulations have similar spectral characteristics. The difference in values representing accuracy is shown in Table 4.

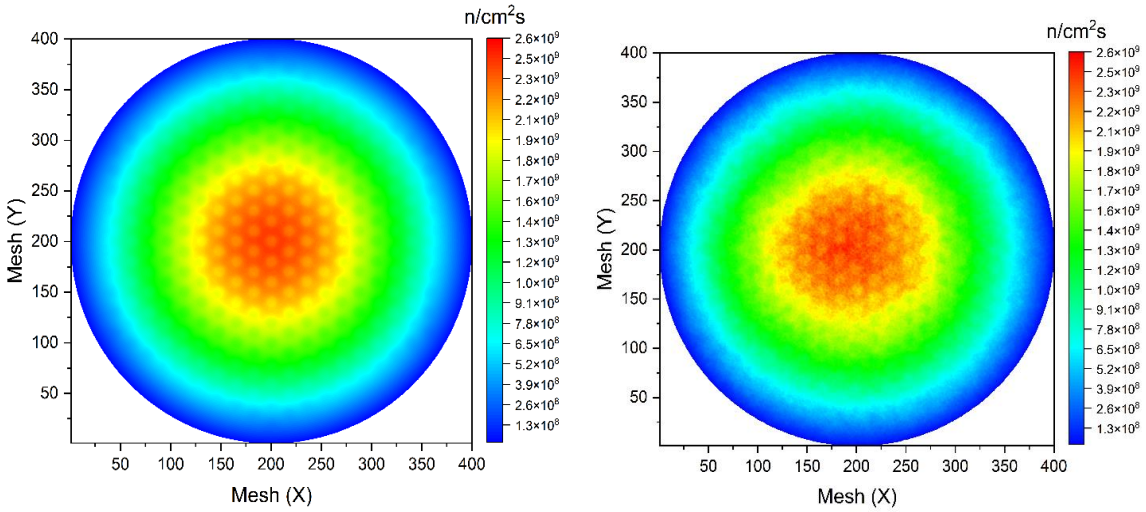

(a) (b)

Figure 8. XY flux distribution for (a) High-Cycle and (b) Low-Cycle.

Figure 8 shows the XY section flux distribution for High-cycle and Low-cycle calculations. The neutron flux in the graphite moderator is higher than the fuel's. The pattern can be seen quite clearly in the two calculation results. The pattern on the Low-Cycle calculation fades more than the High-Cycle calculation. It follows the number of particles and repetitions used. Based on Table 4, the difference in

the level of accuracy is 1:10, so the results in Figure 8 are an interpretation of the difference in the level of accuracy of the two calculations.

4. CONCLUSION

The Low-cycle and Low-particle OpenMC code requires a minimum of 15,000 particles with 100 cycles, comprising 70 active and 30 inactive cycles. A 0.7% error against reference data indicates that the Low-cycle and Low-particle code can maintain accurate calculations, proving beneficial for computations with minimal computational resources. However, the limitation of this research lies in the restricted geometry utilized, specifically the official design of the MSR FUJI-12. In the future, it is essential to investigate whether the findings of this study can be extrapolated to more complex reactor geometry designs.

REFERENCES

Brown, F. B. (2006). On the use of shannon entropy of the fission distribution for assessing convergence of Monte Carlo criticality calculations. *PHYSOR-2006 - American Nuclear Society's Topical Meeting on Reactor Physics*, *2006*, 1–6. https://inis.iaea.org/search/searchsinglerecord.aspx?recordsFor=SingleRecord&RN=43129860

Carney, S., Brown, F., Kiedrowski, B., & Martina, W. (2014). Theory and Applications of the Fission Matrix Method for Continuous-Energy. *Annals of Nuclear Energy*, *73*, 423–431. https://doi.org/https://doi.org/10.1016/j.anucene.2014.07.020

Farkas, G., Petriska, M., Michálek, S., Sluge, V., & Vanková, A. (2017). WWER-440 Criticality Calculations using MCNP5 Code. *18th Symposium of AER on VVER Reactor Physics and Reactor Safety*. https://inis.iaea.org/collection/NCLCollectionStore/_Public/40/059/40059704.pdf

Hursin, M., Vasiliev, A., Rochman, D., Dokhane, A., & Ferroukhi, H. (2024). Monte Carlo analysis of BWR geometries using a cycle check-up methodology. *Annals of Nuclear Energy*, *195*. https://doi.org/10.1016/j.anucene.2023.110170

IAEA. (2016). *Status Report – MSR-FUJI* (IAEA, Ed.). IAEA. https://aris.iaea.org/PDF/MSR-FUJI.pdf

Karomah, I., Mabruri, A. M., Syarifah, R. D., & Trianti, N. (2023). ANALYSIS OF CORE CONFIGURATION FOR CONCEPTUAL GAS COOLED FAST REACTOR (GFR) USING OPENMC. *JURNAL TEKNOLOGI REAKTOR NUKLIR TRI DASA MEGA*, *25*(2), 85. https://doi.org/10.55981/tdm.2023.6879

Kiedrowski, B. C., & Beyer, K. A. (2017). Monte Carlo Fission Source Convergence with Nearest-Neighbor Estimates of the Differential Entropy. *International Conference on Mathematics & Computational Methods Applied to Nuclear Science & Engineering*, *53*(30), 1–23. https://inis.iaea.org/search/search.aspx?orig_q=RN:53074355

Kumala Sari, A., Dewi Syarifah, R., & Arkundato, A. (n.d.). *Preliminary Study of 300 MWth Pressurized Water Reactor with Carbide Fuel with Addition Neptunium 237 Using SRAC-COREBN Code*. https://doi.org/10.1063/5.0108190

Kunlun, D. (2016). *A Monte-Carlo Simulation for Neutron Transport in Spherical Reactor*. National University of Singapore.

Mabruri, A. M., Syarifah, R. D., Aji, I. K., Hanifah, Z., Arkundato, A., & Jatisukamto, G. (2022). Neutronic analysis on molten salt reactor FUJI-12 using 235U as fissile material in LiF-BeF2-UF4 fuel. *Eastern-European Journal of Enterprise Technologies*, *5*(8(119)), 6–12. https://doi.org/10.15587/1729-4061.2022.265798

Mickus, Ignas. (2021). *Towards Efficient Monte Carlo Calculations in Reactor Physics : Criticality, Kinetics and Burnup Problems*. Stockholm, Sweden: KTH Royal Institute of Technology.

Omar, M. R. (2021). An effective mesh-free fission source convergence indicator for Monte Carlo k-Eigenvalue problems. *Nuclear Engineering and Design*, *372*(September), 110960. https://doi.org/10.1016/j.nucengdes.2020.110960

OpenMC. (2023). *The OpenMC Monte Carlo Code*. MIT. https://docs.openmc.org/en/stable/methods/geometry.html

Romano, P. K., Horelik, N. E., Herman, B. R., Nelson, A. G., Forget, B., & Smith, K. (2015). OpenMC: A state-of-the-art Monte Carlo code for research and development. *Annals of Nuclear Energy*, *82*, 90–97. https://doi.org/10.1016/j.anucene.2014.07.048

Souček, P., Beneš, O., Tosolin, A., & Konings, R. (2018). Chemistry of molten salt reactor fuel salt candidates. *Transactions of the American Nuclear Society*, *118*(July), 114–117. https://publications.jrc.ec.europa.eu/repository/handle/JRC110789?mode=full

Suzuki, N., & Shimazu, Y. (2008). Reactivity-initiated-accident analysis without scram of a molten salt reactor. *Journal of Nuclear Science and Technology*, *45*(6), 575–581. https://doi.org/10.1080/18811248.2008.9711881

Syarifah, R. D., Nasrullah, M., Prasetya, F., Mabruri, A. M., Arkundato, A., Jatisukamto, G., & Handayani, S. (2024). Analysis of variation minor actinide pin configurations Np-237, AM-241, and Cm-244 in UN-PuN fueled pressurized water reactor. *EUREKA: Physics and Engineering*, *1*, 36–46. https://doi.org/10.21303/2461-4262.2024.003048

Syarifah, R. D., Su'ud, Z., Basar, K., Irwanto, D., Pattipawaej, S. C., & Ilham, M. (2017a). WITHDRAWN: Comparison of uranium plutonium nitride (U Pu N) and thorium nitride (Th N) fuel for 500 MWth Gas Cooled Fast Reactor (GFR) longlife without refueling. *International Journal of Hydrogen Energy*. https://doi.org/10.1016/j.ijhydene.2017.07.183

Syarifah, R. D., Su'ud, Z., Basar, K., Irwanto, D., Pattipawaej, S. C., & Ilham, M. (2018). Comparison of uranium plutonium nitride (U-Pu-N) and thorium nitride (Th-N) fuel for 500 MWth gas-cooled fast reactor (GFR) long life without refueling. *International Journal of Energy Research*, *42*(1), 214–220. https://doi.org/10.1002/er.3923

Syarifah, R. D., Su'ud, Z., Basar, K., & Irwanto, D. (2020). Actinide Minor Addition on Uranium Plutonium Nitride Fuel for Modular Gas Cooled Fast Reactor. *Journal of Physics: Conference Series*, *1493*(1). https://doi.org/10.1088/1742-6596/1493/1/012020

Syarifah, R. D., Yulianto, Y., Su'ud, Z., Basar, K., & Irwanto, D. (2017b). Neutronic analysis of Thorium Nitride (Th, U233)N fuel for 500MWth Gas Cooled Fast Reactor (GFR) long life without refueling. *Key Engineering Materials*, *733 KEM*, 47–50. https://doi.org/10.4028/www.scientific.net/KEM.733.47

Syarifah, R. D., Aula, M. H., Ardianingrum, A., Janah, L. N., & Maulina, W. (2022). Comparison of thorium nitride and uranium nitride fuel on small modular pressurized water reactor in neutronic analysis using SRAC code. *Eastern-European Journal of Enterprise Technologies*, *2*(8 (116)), 21–28. https://doi.org/10.15587/1729-4061.2022.255849

Syarifah, R. D., Nabhan Mh, N., Hanifah, Z., Karomah, I., Mabruri, A. M., Arkundato, D. A., Fisika, J., Matematika, F., Ilmu, D., Alam, P., & No, J. K. (2021). Analisis Fraksi Volume Bahan Bakar Uranium Karbida Pada Reaktor Cepat Berpendingin Gas Menggunakan SRAC Code. *Jurnal Jaring SainTek (JJST)*, *3*(1), 13–18. http://ejurnal.ubharajaya.ac.id/index.php/jaring-saintek

Vaz, P. (2009). Neutron transport simulation (selected topics). *Radiation Physics and Chemistry*, *78*(10), 829–842. https://doi.org/10.1016/j.radphyschem.2009.04.022

Waris, A., Aji, I. K., Novitrian, Kurniadi, R., & Su'ud, Z. (2012). Plutonium and minor actinides utilization in thorium molten salt reactor. *AIP Conference Proceedings*, *1448*(2012), 115–118. https://doi.org/10.1063/1.4725445

Waris, A., Aji, I. K., Pramuditya, S., Novitrian, Permana, S., & Su'Ud, Z. (2015). Comparative Studies on Plutonium and Minor Actinides Utilization in Small Molten Salt Reactors with Various Powers and Core Sizes. *Energy Procedia*, *71*, 62–68. https://doi.org/10.1016/j.egypro.2014.11.855

Yamaguchi, C. H., Stefani, G. L., & Santos, T. A. (2017). A general overview of generation IV molten salt reactor (MSR) and the use of thorium as fuel. *International Nuclear Atlantic Conference - INAC 2017*. https://inis.iaea.org/collection/NCLCollectionStore/_Public/48/103/48103603.pdf